Tetrahedron 74 (2018) 4259–4265

Contents lists available at ScienceDirect

Tetrahedron

journal homepage: www.elsevier.com/locate/tet

COX-2 and JAK3 inhibitory meroterpenoids from the mushroom *Ganoderma theaecolum*

Qi Luo [b, d], Min-Ke Li [c], Jing-Feng Luo [c], Zheng-Chao Tu [c, **], Yong-Xian Cheng [a, *]

[a] Guangdong Key Laboratory for Genome Stability & Disease Prevention, School of Pharmaceutical Sciences, Shenzhen University Health Science Center, Shenzhen, 518060, PR China
[b] State Key Laboratory of Phytochemistry and Plant Resources in West China, Key Laboratory for Plant Diversity and Biogeography of East Asia, Kunming Institute of Botany, Chinese Academy of Sciences, Kunming, 650201, PR China
[c] Drug Discovery Pipeline & Guangdong Provincial Key Laboratory of Biocomputing, Guangzhou Institutes of Biomedicine and Health, Guangzhou, 510530, PR China
[d] University of Chinese Academy of Sciences, Beijing, 100049, PR China

ARTICLE INFO

Article history:
Received 10 May 2018
Received in revised form
19 June 2018
Accepted 20 June 2018
Available online 22 June 2018

Keywords:
Ganoderma theaecolum
Meroterpenoids
Ganotheaecolumols A–K
COX-2
JAK3

ABSTRACT

Ganoderma mushrooms possess antioxidant, anticancer, and immunomodulatory properties. In this study, eleven new meroterpenoids, ganotheaecolumols A-K (**1**–**6**, **10**,**11**, **13**, **14**, and **17**), together with nine known ones (**7**–**9**, **12**, **15**, **16**, and **18**–**20**) were isolated from the fruiting bodies of *G. theaecolum*. Their structures were elucidated by spectroscopic and computational methods. All the new compounds and iso-ganotheaecolumol I (**12**) were tested for their inhibitory activities against COX-2 and JAK3 kinases, and cytotoxic effects. It was found that most meroterpenoids could inhibit COX-2 and JAK3 with compounds **3**, **4**, **12**, **13**, and **17** having IC_{50} values of 1.05 ± 0.10, 1.38 ± 0.11, 2.61 ± 0.79, 3.47 ± 0.58, and 4.84 ± 0.60 μM towards COX-2. Whereas, none of the test compounds exhibited cytotoxic effects against human cancer cells (K562, A549, and Huh-7).

1. Introduction

Ganoderma lingzhi (*G. lucidum*) and *G. sinensis* are well-known mushrooms, which are widely used as effective medicines and health food stuff exemplified by rice wine [1], sour milk [2], or tea in East Asia [3]. In the past 60 years, triterpenoids in *Ganoderma* mushrooms were thoroughly studied especially on their antioxidant, anticancer and immunomodulatory activities [4,5]. However, recent studies pioneered by us revealed lots of meroterpenoids from *Ganoderma* mushrooms. *G. theaecolum* in folk are used as fermented delicious foods or a substitute of *G. lingzhi* for treating and preventing chronic diseases [6]. So far, only several triterpenoids with antitumor and liver protection properties were documented [7,8]. Our previous study on the title mushroom revealed the presence of a new carbon skeleton steroid possessing neurotrophic activity and a series of terminal cyclohexane-type meroterpenoids [6,9]. As a follow-up chemical investigation on this fungal species targeting meroterpenoids biogenetically featuring hybridization of a shikimic acid and a mevalonic acid, twenty meroterpenoids including eleven new ones were isolated and structurally identified (Fig. 1), their biological activities against cyclooxygenase 2 (COX-2), Janus kinase 3 (JAK3), and human cancer cells (K562, A549 and Huh-7) were evaluated.

2. Results and discussion

2.1. Structure elucidation

(-)-Ganotheaecolumol A (**1**) has the molecular formula $C_{21}H_{26}O_6$ derived by analysis of its negative HRESIMS. The ^{1}H NMR spectrum (Table 1) contains an ABX spin system [δ_H 7.11 (1H, d, $J = 2.3$ Hz, H-3), 7.02 (1H, dd, $J = 8.9$, 2.3 Hz, H-5), and 6.95 (1H, d, $J = 8.9$ Hz, H-6)], two olefinic protons and two methyl signals. The ^{13}C NMR and DEPT spectra display 21 carbons including two methyls, six aliphatic methylenes (one oxygenated), five methines (sp^2), one ketone, one carboxylic acid, five sp^2 carbons, and one oxygenated quaternary carbon. The ^{1}H-^{1}H COSY spectrum shows the

* Corresponding author.
** Corresponding author.
E-mail addresses: tu_zhengchao@gibh.ac.cn (Z.-C. Tu), yxcheng@szu.edu.cn (Y.-X. Cheng).

https://doi.org/10.1016/j.tet.2018.06.053
0040-4020/

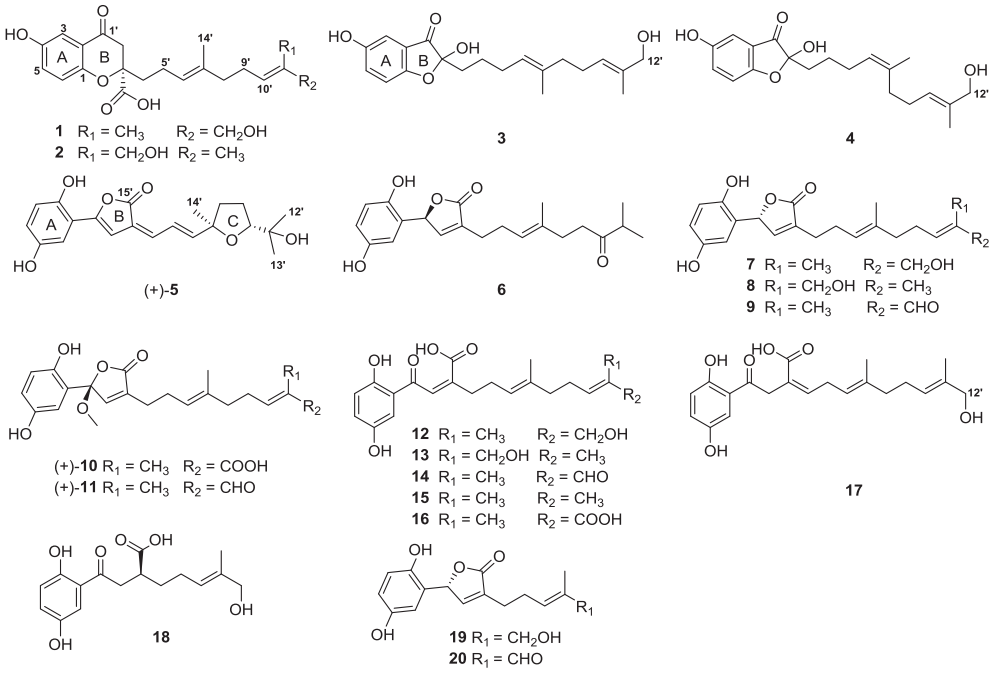

Fig. 1. The chemical structures of compounds **1**–**20**.

Table 1
^{1}H NMR (600 MHz) and ^{13}C NMR (150 MHz) spectral data of compounds **1**–**5** in methanol-d_4 (δ in ppm).

No.	**1**		**2**		**3**		**4**		**5**	
	δ_H (J in Hz)	δ_C	δ_H (J in Hz)	δ_C	δ_H (J in Hz)	δ_C	δ_H (J in Hz)	δ_C	δ_H (J in Hz)	δ_C
1		155.8		155.9		166.4		166.4		151.1
2		122.0		122.0		120.9		120.9		116.5
3	7.11 d (2.3)	110.9	7.11 d (2.3)	110.9	6.92 d (2.7)	108.5	6.92 d (2.7)	108.6	7.06 d (2.8)	113.3
4		152.9		152.8		153.8		153.8		151.2
5	7.02 dd (8.9, 2.3)	125.9	7.02 dd (8.9, 2.3)	125.9	7.20 dd (8.9, 2.7)	129.3	7.20 dd (8.9, 2.7)	129.3	6.70 dd (8.8, 2.8)	119.1
6	6.95 d (8.9)	120.5	6.95 d (8.9)	120.6	6.95 d (8.9)	114.9	6.95 d (8.9)	114.9	6.76 overlap	117.6
1′		193.7		193.8		202.7		202.7		153.5
2′	Ha: 3.09 d (16.3) Hb: 2.89 d (16.3)	45.5	Ha: 3.10 d (16.3) Hb: 2.88 d (16.3)	45.6		107.1		107.1	7.10 s	105.2
3′		85.6[a]		85.8[a]	1.84 m	36.3	1.83 m	36.5		128.2
4′	1.97 m	39.0	1.96 m	39.0	Ha: 1.42 m Hb: 1.25 m	23.9	Ha: 1.41 m Hb: 1.25 m	24.2	6.99 d (11.9)	135.1
5′	Ha: 2.25 m Hb: 2.13 m	23.2	Ha: 2.25 m Hb: 2.12 m	23.2	1.97 m	28.7	1.97 m	28.7	6.75 overlap	124.3
6′	5.17 t (5.8)	124.5	5.16 t (5.7)	124.6	5.06 t (6.8)	125.3	5.08 t (7.3)	126.0	6.43 d (15.0)	152.6
7′		137.0		136.9		136.5		136.7		84.5
8′	2.03 t (7.5)	40.4	2.01 t (7.6)	41.0	2.02 m	40.5	2.03 m	32.5	Ha: 1.99 m Hb: 1.85 m	38.7
9′	2.15 m	27.2	2.16 m	27.1	2.13 m	27.2	2.09 m	27.2	1.90 m	27.5
10′	5.38 t (6.8)	126.4	5.25 t (7.1)	128.4	5.35 t (6.9)	126.5	5.38 t (6.6)	126.5	3.88 t (6.8)	87.4
11′		136.0		135.8		136.0		136.1		72.5
12′	3.91 s	68.9	4.05 s	61.4	3.89 s	69.0	3.91 s	69.0	1.20 s	25.5
13′	1.64 s	13.7	1.75 s	21.5	1.62 s	13.7	1.64 s	13.7	1.22 s	25.9
14′	1.63 s	16.1	1.62 s	16.0	1.57 s	16.1	1.67 s	23.6	1.40 s	27.1
15′		176.4[a]		176.8[a]						170.4

[a] Assigned by the HMBC experiment.

correlations of H-5/H-6, H-4′/H-5′/H-6′, and H-8′/H-9′/H-10′. These data demonstrate that **1** is similar to ganoresinain B [10]. However, the tailing behavior on TLC suggests that **1** might contain a free carboxylic acid group. The HMBC experiment exhibits correlations of H-2′/C-2, C-1′, C-3′, C-4′, C-15′, combining with the chemical shift of C-3′ (δ_C 85.6) and 9 degrees of unsaturation, indicating that C-3′ is connected to C-1 via an oxygen bridge to form ring B. Significant ROESY correlations of H-6′/H-8′ and H-10′/H-12′ suggested that two double bonds ($\Delta^{6'(7')}$ and $\Delta^{10'(11')}$) are both *E*-form.

In order to determine the absolute configuration at C-3′, electronic circular dichroism (ECD) calculations were carried out. The ECD spectrum of (3′*R*)-**1** agrees well with the experimental CD spectrum of (-)-**1**, leading to the unambiguous assignment of the absolute configuration as 3′*R* (Fig. 2).

Detailed interpretation of NMR data of (-)-ganotheaecolumol B (**2**) and **1** found the configurational difference of their double bond $\Delta^{10'(11')}$, whose *Z*-form is supported by the ROESY correlation of H-10′/H-13′ (Fig. 3). Likewise, the absolute configuration of (-)-**2** was

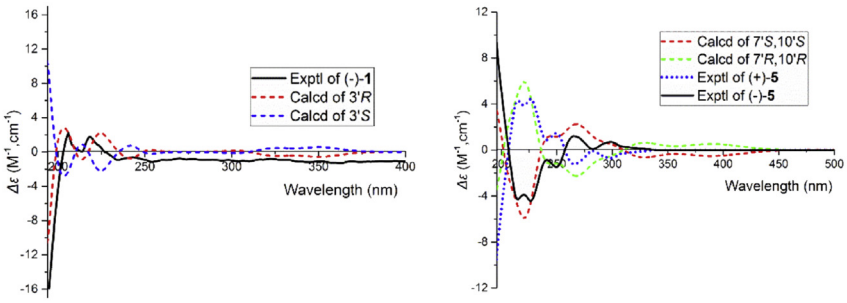

Fig. 2. Comparison of the calculated ECD spectra with the experimental spectra of compounds (-)-**1** and (±)-**5** in MeOH at B3LYP/6-311G(d,p) level.

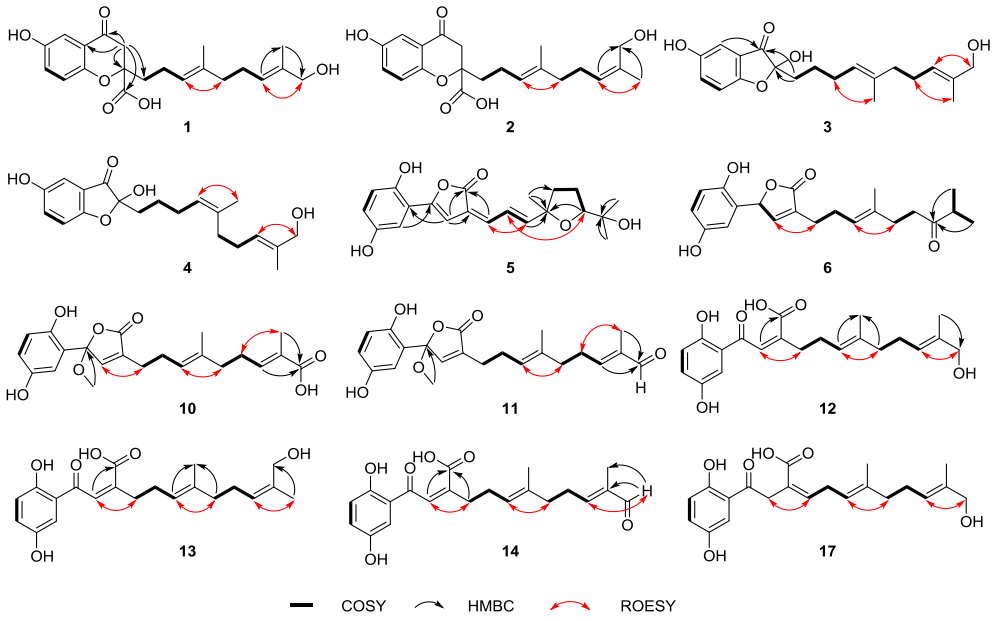

Fig. 3. Key ^{1}H-^{1}H COSY, HMBC, and ROESY correlations of compounds **1**–**6**, **10**–**14**, and **17**.

assigned as 3′*R* based on their extreme similarity of experimental CD curves (see supplementary data).

The HRESIMS of (±)-ganotheaecolumol C (**3**) gives a quasimolecular ion peak at *m*/*z* 459.1629 [M + CF_3COO]$^-$, in accordance with the molecular formula $C_{20}H_{26}O_5$. The ^{1}H and ^{13}C NMR data of **3** resemble those of **1**, except for the difference of ring B. This conclusion is supported by the HMBC correlations of H-3/C-1′ (δ_C 202.7) and H-3′/C-1′, C-2′ (δ_C 107.1), and the chemical shift of C-1 (δ_C 166.4). In addition, a detailed interpretation of 1D NMR data between **3** and **4** indicates that they are analogues, only differing from the configuration of $\Delta^{6'(7')}$ double bond, *E*-form for **3** was determined from key ROESY correlation of H-5′/H-14′, in contrast, *Z*-form of $\Delta^{6'(7')}$ double bond for **4** was assigned by key ROESY correlation of H-6′/H-14′. The lack of an optical rotation and the plain experimental CD curves of **3** and **4** indicates that both are racemic. We thus tried to separate to yield their enantiomers by using Daicel Chiralpak AD-H and IC chiral HPLC, however, their chromatogram both appears as a single peak, so that it is difficult to determine their absolute configurations. Taken together, (±)-**3** and (±)-ganotheaecolumol D (**4**) were elucidated as shown (Fig. 1).

(±)-Ganotheaecolumol E (**5**) has the molecular formula $C_{21}H_{24}O_6$ (10 degrees of unsaturation) deduced from analysis of its HRESIMS data. The ^{1}H NMR spectrum of **5** (Table 1) contains seven olefinic protons. The ^{13}C NMR and DEPT spectra reveal 21 carbons. Considering meroterpenoids have been characterized from *Ganoderma*, these data suggest **5** to be a meroterpenoid analogue. The structural elucidation of **5** was made mainly by analysis of HMBC data. The existence of ring B is supported by the key HMBC correlations of H-3/C-1′ and H-2′/C-1′, C-3′, C-15′ as well as the chemical shifts of C-1′ (δ_C 153.5), C-2′ (δ_C 105.2), C-3′ (δ_C 128.2), and C-15′ (δ_C 170.4). Meanwhile, the presence of ring C is evidenced by ^{1}H-^{1}H COSY correlations of H-8′/H-9′/H-10′, HMBC correlations of H-10′/C-7′, H_3-14′/C-7′, C-8′ and the chemical shift of C-7′ (δ_C 84.5) and C-10′ (δ_C 87.4). In addition, the chemical shift of C-11′ and HMBC correlations of H_3-12′, H_3-13′/C-11′reveal the feature of the terminal at the side chain. Finally, ^{1}H-^{1}H COSY correlations of H-4′/H-5′/H-6′ and HMBC correlations of H-4′, H-5′/C-3′, H-5′, H-6′/C-7′ allow rings B and C to be connected. The ROESY correlations of H-2′/H-4′ and H-4′/H-6′ suggest that the geometry of $\Delta^{3'(4')}$ double bond is *Z*-form, and that of $\Delta^{5'(6')}$ is *E*-form. Furthermore, the relative configuration of ring C was assigned by key ROESY correlation of H-5′/H-10′. Compound **5**, which is also racemic, was subjected to chiral HPLC to afford the enantiomers, whose absolute configurations at the stereogenic centers were assigned to be 7′*R*,10′*R* for (+)-**5** by using ECD computational methods (Fig. 2). Naturally, the absolute configuration of (-)-**5** was assigned to be 7′*S*,10′*S*.

(-)-Ganotheaecolumol F (**6**) has the molecular formula $C_{21}H_{26}O_5$ deduced from its HRESIMS at *m*/*z* 357.1693, indicating 9 degrees of unsaturation. The ^{1}H and ^{13}C NMR data of **6** are extremely similar to those of **7**. The difference is that the double bond $\Delta^{10'(11')}$ in **7** is

oxygenated to a ketone and the presence of a sp^3 methine. This is supported by key HMBC correlations of H-11′, H-12′, H-13′/C-10′ (δ_C 217.2) and ^{1}H-^{1}H COSY correlations of H-12′/H-11′/H-13′. There is one chiral center in **6**, whose absolute configuration was assigned as 1′*S* based on comparing its specific optical rotation $[\alpha]_D^{24}$ −18.5 (*c* 0.20, MeOH) with that of (-)-zizhine A {$[\alpha]_D^{24}$ −67.4 (*c* 0.26, MeOH) for 1′*S*} [11]. Hence, the structure of **6** was identified.

(±)-Ganotheaecolumol G (**10**) has the molecular formula $C_{22}H_{26}O_7$ (10 degrees of unsaturation) based on analysis of its HRESIMS at *m/z* 401.1609 $[M-H]^-$. The NMR data of **10** (Table 2) resemble those of fornicin B [12] with the exception of the terminal methyl is replaced by a carboxylic acid group, which is confirmed by the key HMBC correlations of H-10′, H-13′/C-12′ (δ_C 172.5). In addition, ROESY correlations of H-6′/H-8′ and H-9′/H-13′ reveal that $\Delta^{6'(7')}$ and $\Delta^{10'(11')}$ double bonds are both *E* configuration. Racemic **10** was subjected to chiral HPLC to afford a pair of enantiomers, whose absolute configurations were determined to be 1′*R* for (+)-**10** and 1′*S* for (-)-**10**, by comparing the experimental value of optical rotation {$[\alpha]_D^{25}$ +53.1 (*c* 0.05, MeOH) for (+)-**10**} with that of calculated one {$[\alpha]_D^{25}$ +51.8}.

Comparison NMR data of ganotheaecolumol H (**11**) with those of **10** found their structure resemblance, differing in that the absence of a carboxylic acid signal at C-12′ (δ_C 172.5) in **11** instead of the presence of an aldehyde group at δ_C 197.3 in **10**. This alteration is supported by HMBC correlation of H-12′/C-11′, C-13′. Compound **11** is also racemic, chiral HPLC separation afforded the enantiomers. Likewise, the absolute configuration of each enantiomer [(+)-**11** is 1′*R* and (-)-**11** for 1′*S*)] was assigned by comparing their specific optical rotation with those of **10**.

Ganotheaecolumol I (**13**) has the molecular formula $C_{21}H_{26}O_6$ (9 degrees of unsaturation) on the basis of HRESIMS at *m/z* 373.1649 $[M-H]^-$ analysis. The ^{1}H and ^{13}C NMR spectra (Table 2) suggest that the structure of **13** resembles that of ganomycin C (**15**) [13], with the only difference from the terminal methyl in **15** being reduced to a hydroxymethyl group. In addition, the detailed analysis found that the difference between ganotheaecolumol J (**14**) (Table 3) and **12** is that the terminal hydroxymethyl group in **12** is oxidized to an aldehyde group in **14**. This conclusion is supported via the key HMBC correlations of H-12′ (δ_H 9.31)/C-10′, C-11′, C-13′.

Table 3
^{1}H and ^{13}C NMR spectral data of compounds **14** and **17** in methanol-d_4 (δ in ppm).

No.	**14**[a]		**17**[b]	
	δ_H (*J* in Hz)	δ_C	δ_H (*J* in Hz)	δ_C
1		157.7		156.5
2		122.0		120.6
3	7.18 d (2.9)	116.4	7.36 d (2.9)	115.7
4		151.3		150.7
5	7.02 dd (8.9, 2.9)	126.9	7.01 dd (8.9, 2.9)	125.8
6	6.83 d (8.9)	120.4	6.80 d (8.9)	119.7
1′		199.7		204.5
2′	7.61 s	131.2	4.08 s	37.2[c]
3′		150.2[c]		121.8
4′	2.71 dd (15.6, 7.7)	30.0	6.98 t (7.5)	144.9
5′	2.24 m	29.0	2.90 t (7.3)	28.8
6′	5.13 t (6.8)	125.9	5.15 t (6.9)	121.4
7′		136.7		138.3
8′	2.03 t (7.5)	39.3	2.03 m	40.3
9′	2.37 m	28.8	2.13 m	27.1
10′	6.51 t (7.2)	157.2	5.37 t (6.7)	126.3
11′		141.0		136.1
12′	9.31 s	197.7	3.90 s	69.0
13′	1.67 s	9.6	1.63 s	13.7
14′	1.61 s	16.6	1.63 s	16.3
15′		172.9[c]		171.7[c]

[a] Recorded at 600 (150) MHz.
[b] Recorded at 800 (200) MHz.
[c] Assigned by the HMBC experiment.

Ganotheaecolumol K (**17**) has the molecular formula $C_{21}H_{26}O_6$ (9 degrees of unsaturation) based on its HREIMS. Its ^{1}H and ^{13}C NMR spectra are closely related to those of **12**. The only change is the presence of a $\Delta^{3'(4')}$ instead of a $\Delta^{2'(3')}$ double bond, supported by the key ^{1}H-^{1}H COSY correlations of H-4′ (δ_H 6.98)/H-5′/H-6′. The ROESY correlation of H-2′/H-4′ evidently suggest the geometry of the $\Delta^{3'(4')}$ to be *Z*-form.

Nine known meroterpenoids were isolated and elucidated as zizhine A (**7**) [11], ganoresinain B (**8**) [10], ganoleucin C (**9**) [14], isoganotheaecolumol I (**12**) [15], ganomycin C (**15**) [13], ganocalidin D (**16**) [16], applanatumols S (**18**) and U (**19**) [17], and chizhine E (**20**)

Table 2
^{1}H NMR (600 MHz) and ^{13}C NMR (150 MHz) spectral data of compounds **6**, and **10**–**13** in methanol-d_4 (δ in ppm).

No.	**6**		**10**		**11**		**12**		**13**	
	δ_H (*J* in Hz)	δ_C	δ_H (*J* in Hz)	δ_C	δ_H (*J* in Hz)	δ_C	δ_H (*J* in Hz)	δ_C	δ_H (*J* in Hz)	δ_C
1		148.9		149.3		149.3		157.2		157.2
2		123.6		123.5		123.5		121.4		121.5
3	6.46 d (2.8)	113.2	6.92 br s	114.6	6.91 br s	114.6	7.16 d (2.7)	115.8	7.17 d (2.7)	115.9
4		151.5		151.2		151.2		150.8		150.8
5	6.61 dd (8.6, 2.8)	117.1	6.67 overlap	118.2	6.67 overlap	118.2	7.04 dd (8.9, 2.7)	126.5	7.03 dd (8.9, 2.7)	126.4
6	6.68 d (8.6)	117.1	6.67 overlap	118.3	6.67 overlap	118.3	6.84 d (8.9)	119.9	6.83 d (8.9)	119.9
1′	6.23 br s	79.8		108.6		108.6		199.0		199.1
2′	7.34 br s	151.3	7.40 s	148.4	7.42 s	148.5	7.66 s	132.1	7.63 s	131.3[a]
3′		132.8		135.6		135.6		147.3[a]		148.6[a]
4′	2.34 m	26.0	2.34 m	25.9	2.35 overlap	25.8	2.70 t (7.2)	29.3	2.68 t (7.3)	29.5
5′	2.29 m	26.8	2.27 m	26.7	2.29 m	26.7	2.22 m	28.6	2.21 m	28.6
6′	5.12 t (6.5)	124.4	5.11 t (6.9)	124.5	5.12 t (6.8)	124.8	5.08 t (7.0)	124.3	5.09 t (7.0)	124.5
7′		136.9		137.2		136.8		137.3		137.1
8′	2.17 t (7.8)	34.5	2.00 t (7.5)	39.3	2.09 t (7.5)	38.9	1.86 t (7.6)	40.2	1.84 t (7.6)	40.8
9′	2.50 t (7.8)	40.1	2.14 m	28.2	2.35 overlap	28.4	2.02 m	27.1	2.06 m	27.0
10′		217.2	6.67 overlap	142.9	6.52 t (7.2)	156.6	5.31 t (6.7)	126.6	5.18 t (7.1)	128.5
11′	2.63 m	41.8		129.3[a]		140.5		135.8		135.6
12′	1.05 d (3.3)	18.6		172.5	9.32 s	197.3	3.88 s	69.0	4.02 s	61.4
13′	1.03 d (3.3)	18.6	1.78 s	12.6	1.69 s	9.1	1.60 s	13.7	1.72 s	21.5
14′	1.57 s	16.3	1.51 s	16.1	1.53 s	16.0	1.56 s	16.1	1.56 s	16.1
15′		176.8		173.4		173.4		171.0[a]		171.0[a]
16′			3.27 s	52.2	3.26 s	52.3				

[a] Assigned by the HMBC experiment.

[18] by comparing their spectroscopic data with those previously reported for these substances. For compound **12**, its NMR data have not been previously reported, we will add them in Table 2.

2.2. Biological evaluation

The isolated meroterpenoids, except for the known ones (**7**–**9**, **15**, **16**, and **18**–**20**), were evaluated for their inhibitory activities against COX-2 and JAK3 kinases and cytotoxic property. It was found that compounds **3**, **4**, **12**, **13**, and **17** show potent COX-2 inhibitory activities with IC_{50} values of 1.05 ± 0.10, 1.38 ± 0.11, 2.61 ± 0.79, 3.47 ± 0.58, and 4.84 ± 0.60 μM, respectively. Others (-)-**6**, **10**–**14**, and **17** also display certain inhibitory activities against COX-2 (Table 4). The biological difference between **1**–**4** toward COX-2 suggests that the importance of benzofuran moiety for keeping the activity. Analysis of structures **10**–**13**, **14**, and **17** found that the five-membered lactone moiety in **10** and **11** might be transformed into the structure part consisting of C-7'–C-10′ in **12**–**17**. In this sense, it is not strange that these compounds all exhibit inhibitory activity against COX-2. This might be also the reasons that meroterpenoids (-)-**6**, (+)-**10**, (-)-**10**, (+)-**11**, **12**–**14**, and **17** all show certain significant inhibitory activities against JAK3 despite that their side chains are different. Finally, none of the test compounds exhibit cytotoxic effects on the three cancer lines (K562, A549 and Huh-7).

In summary, eleven new meroterpenoids, ganotheaecolumols A-K (**1**–**6**, **10**, **11**, **13**, **14**, and **17**), together with nine known ones were isolated from the fruiting bodies of the mushroom *G. theaecolum*. The structurally diverse meroterpenoids are characteristic of several types such as benzopyran-, benzofuran- and long side chain-types. In addition to compounds **3** and **4**, the absolute configurations of all the other new ones were clarified by spectroscopic analysis, optical rotation or ECD calculations. Biological evaluation of all the new compounds reveals that most such meroterpenoids are active towards COX-2 and JAK3 inhibition but not active in human cancer cells. COX-2 and JAK3 are implicated in multiple acute or chronic disorders such as inflammation, diabetic nephropathy, blood disease and rheumatoid arthritis [19], our previous study also disclosed that meroterpenoids from *Ganoderma* species could activate Nrf2 showing antioxidant property [20,21], therefore, the present findings will pave the way for developing *Ganoderma* fungi exemplified by *G. theaecolum* as healthcare foods.

Table 4
Inhibitory activities of the tested compounds for COX-2 and JAK3 kinases.

Compounds	IC_{50} (μM)	
	COX-2	JAK3
(-)-**1**	NA	NA
(-)-**2**	NA	NA
3	1.05 ± 0.10	>30
4	1.38 ± 0.11	>30
(+)-**5**	NA	NA
(-)-**5**	NA	NA
(-)-**6**	6.32 ± 0.73	10.36 ± 1.06
(+)-**10**	7.35 ± 0.44	13.83 ± 0.37
(-)-**10**	8.17 ± 0.65	8.86 ± 3.48
(+)-**11**	11.16 ± 0.89	24.38 ± 7.58
(-)-**11**	NA	NA
12	2.61 ± 0.79	15.64 ± 10.17
13	3.47 ± 0.58	11.18 ± 0.47
14	6.59 ± 0.10	7.55 ± 1.20
17	4.84 ± 0.60	3.63 ± 0.56
Celecoxib	0.0087 ± 0.0004	/
Staurosporine	/	0.00047 ± 0.00002

NA: no activity.

3. Materials and methods

3.1. General

UV spectra were collected on a Shimadzu UV2401PC spectrometer. Optical rotations were recorded on a Jasco P-1020 digital polarimeter. ESIMS and HRESIMS were measured on an Agilent 1290 UPLC/6540 Q-TOF instrument. CD spectra were measured on an Applied Photophysics Chirascan instrument. NMR spectra were measured on a Bruker AV 600 or 800 MHz spectrometer, with TMS as an internal standard. RP-18 (40–63 μm, Daiso Co., Japan), MCI gel CHP 20P (75–150 μm, Tokyo, Japan), silica gel GF254 (80–100 mesh, Qingdao Marine Chemical Inc., P.R. China), and Sephadex LH-20 (Amersham Biosciences, Sweden) were used for column chromatography. Semi-preparative HPLC was carried out using an Agilent 1200 liquid chromatograph and a LC-3000 high liquid chromatograph (P.R. China), the columns used were YMC-Pack ODS-A (25 mm × 10 mm, i.d., 5 μm) and Daicel Chiralpak IC (250 mm × 10 mm, i.d., 5 μm), flow rate: 2.5 mL/min; and Daicel Chiralpak AD-H (250 mm × 4.6 mm, i.d., 5 μm), flow rate: 1.0 mL/min.

3.2. Fungal material

The fruiting bodies of *G. theaecolum* were purchased from a market of Chinese medical material named Zhonghao-Luoshi-Wan of Kunming, Yunnan province, P.R. China, in October 2014. The material was identified by Prof. Zhu-Liang Yang at Kunming Institute of Botany, Chinese Academy of Sciences, P.R. China, and a voucher specimen (CHYX-0603) was deposited at the School of Pharmaceutical Sciences, Shenzhen University Health Science Center, P.R. China since October 2017.

3.3. Extraction and isolation

Dried and powdered *G. theaecolum* fruits (37.5 kg) was extracted with aqueous EtOH (80%, 2 × 150 L × 2 h) to give a crude extract, which was suspended in H_2O followed by extraction with EtOAc to afford an extract (0.85 kg). The EtOAc extract was divided into nine parts (Fr.1–Fr.9) by using a MCI gel CHP 20P column eluted with aqueous MeOH (20%–100%). Fr.4 (58.2 g) was fractionated by a MCI gel CHP 20P column eluted with aqueous MeOH (30%–60%) to provide seven portions (Fr.4.1–Fr.4.7). Of these, Fr.4.3 (32.0 g) was subjected to sequential Sephadex LH-20 (MeOH) to yield two parts (Fr.4.3.1 and Fr.4.3.2). Fr.4.3.2 (6.0 g) was divided into eight fractions (Fr.4.3.2.1–Fr.4.3.2.8) by a RP-18 column eluted with aqueous MeOH (27%). Fr.4.3.2.7 (1.8 g) was firstly filtered using Sephadex LH-20 (MeOH), and then purified by semi-preparative HPLC to afford compound **19** (3.0 mg, $t_R = 14.5$ min, CH_3CN:H_2O, 42:58). Fr.4.4 (5.2 g) was separated to yield seven fractions, of which, Fr.4.4.5 (0.8 g) was subjected to Sephadex LH-20 (MeOH) followed by semi-preparative HPLC to gain compound **20** (2.6 mg, $t_R = 25.4$ min, MeOH:H_2O:HCOOH, 52:48:0.01%). Fr.7 (125.0 g) was separated by a MCI gel CHP 20P column eluted with aqueous MeOH (50%–70%) to afford eleven portions (Fr.7.1–Fr.7.11). Fr.7.6 (8.1 g) was submitted to Sephadex LH-20 (MeOH) to produce four parts (Fr.7.6.1–Fr.7.6.4). Compounds **1** (3.0 mg, $t_R = 18.8$ min) and **2** (3.0 mg, $t_R = 22.3$ min) were successively isolated from Fr.7.6.2 (1.0 g) by using semi-preparative HPLC (CH_3CN:H_2O:HCOOH, 42:58:0.01%). Fr.7.9 (13.8 g) was divided into four portions (Fr.7.9.1–Fr.7.9.4) by Sephadex LH-20 (MeOH). Compounds **18** (2.0 mg, $t_R = 15.0$ min), **9** (5.6 mg, $t_R = 16.3$ min), and **8** (3.0 mg, $t_R = 16.4$ min) were purified from Fr.7.9.2 (4.0 g) by a RP-18 column eluted with aqueous MeOH (40%–50%) followed by semi-preparative HPLC (MeOH:H_2O:HCOOH, 65:35:0.01%). Removal of

abundant triterpenoids from Fr.8 (48.7 g) by Sephadex LH-20 (MeOH) to afford one fraction (5.8 g), which was subsequently subjected to a RP-18 column eluted with aqueous MeOH (50%–70%) to afford seven portions (Fr.8.1–Fr.8.7). Among them, Fr.8.6 (2.3 g) was submitted to Sephadex LH-20 (MeOH) to yield three parts (Fr.8.6.1–Fr.8.6.3). Compounds **14** (2.0 mg, $t_R = 14.6$ min), **6** (3.0 mg, $t_R = 15.7$ min), **10** (2.5 mg, $t_R = 21.6$ min), and **5** (3.5 mg, $t_R = 23.3$ min) were purified from Fr. 8.6.2 (1.0 g) by semi-preparative HPLC (CH_3CN:H_2O:HCOOH, 50:50:0.01%). Compounds **17** (2.0 mg, $t_R = 16.3$ min), **3** (2.2 mg, $t_R = 16.8$ min), and **4** (3.0 mg, $t_R = 19.3$ min) were separated from Fr. 8.7 (0.1 g) by using Sephadex LH-20 (MeOH) and final semi-preparative HPLC (CH_3CN:H_2O, 50:50). Likewise, the abundant triterpenoids in Fr.9 (50.0 g) was removed by Sephadex LH-20 (MeOH) to afford one fraction (5.1 g), which was subsequently subjected to a RP-18 column eluted with aqueous MeOH (60%–100%) to obtain eleven portions (Fr.9.1–Fr.9.11). Compounds **11** (1.4 mg, $t_R = 15.0$ min) and **7** (2.0 mg, $t_R = 17.0$ min) were purified from Fr. 9.4 (0.1 g) by semi-preparative HPLC (MeOH:H_2O, 75:25). Fr.9.6 (8.1 g) was eluted by Sephadex LH-20 (MeOH) followed by semi-preparative HPLC (CH_3CN:H_2O:HCOOH, 55:45:0.01%) to produce compounds **12** (1.0 mg, $t_R = 13.3$ min), **16** (1.0 mg, $t_R = 15.3$ min), and **13** (1.5 mg, $t_R = 17.4$ min). Finally, Fr.9.6 (15.0 mg) was purified by semi-preparative HPLC (MeOH:H_2O:HCOOH, 84:16:0.01%) to afford compound **15** (3.0 mg, $t_R = 12.4$ min).

3.3.1. (-)-Ganotheaecolumol A (**1**)

Yellow gum; $[\alpha]_D^{24}$ −19.7 (*c* 0.26, MeOH); UV (MeOH) λ_{max} (log ε) 360 (3.25), 254 (3.56), 225 (3.97), 204 (4.08) nm; CD (MeOH) $\Delta\varepsilon_{206}$ +2.20, $\Delta\varepsilon_{218}$ +1.75; ESIMS *m/z* 373 $[M-H]^-$, HRESIMS *m/z* 373.1661 $[M-H]^-$ (calcd for $C_{21}H_{25}O_6$, 373.1657).

3.3.2. (-)-Ganotheaecolumol B (**2**)

Yellow gum; $[\alpha]_D^{24}$ −4.0 (*c* 0.25, MeOH); UV (MeOH) λ_{max} (log ε) 361 (3.31), 254 (3.64), 226 (4.05), 205 (4.23) nm; CD (MeOH) $\Delta\varepsilon_{203}$ +4.40; ESIMS *m/z* 373 $[M-H]^-$, HRESIMS *m/z* 373.1661 $[M-H]^-$ (calcd for $C_{21}H_{25}O_6$, 373.1657).

3.3.3. (±)-Ganotheaecolumol C (**3**)

Yellow gum; $[\alpha]_D^{26}$ −1.5 (*c* 0.50, MeOH); UV (MeOH) λ_{max} (log ε) 383 (3.42), 258 (3.75), 205 (4.23) nm; ESIMS *m/z* 345 $[M-H]^-$, HRESIMS *m/z* 459.1629 $[M + CF_3COO]^-$ (calcd for $C_{22}H_{26}F_3O_7$ 459.1636).

3.3.4. (±)-Ganotheaecolumol D (**4**)

Yellow gum; $[\alpha]_D^{24}$ +0.7 (*c* 0.14, MeOH); UV (MeOH) λ_{max} (log ε) 381 (3.54), 257 (3.88), 205 (4.31) nm; ESIMS *m/z* 345 $[M-H]^-$, HRESIMS *m/z* 345.1705 $[M-H]^-$ (calcd for $C_{20}H_{25}O_5$ 345.1707).

3.3.5. (±)-Ganotheaecolumol E (**5**)

Yellow gum; UV (MeOH) λ_{max} (log ε) 362 (3.45), 263 (4.29), 228 (4.11), 197 (4.05) nm; {$[\alpha]_D^{25}$ +28.2 (*c* 0.06, MeOH); CD (MeOH) $\Delta\varepsilon_{215}$ +4.44, $\Delta\varepsilon_{225}$ +4.47, $\Delta\varepsilon_{268}$ −1.25; (+)-**5**}; {$[\alpha]_D^{25}$ −30.0 (*c* 0.13, MeOH); CD (MeOH) $\Delta\varepsilon_{214}$ −4.47, $\Delta\varepsilon_{226}$ −4.48, $\Delta\varepsilon_{267}$ +1.27; (-)-**5**}; ESIMS *m/z* 371 $[M-H]^-$, HRESIMS *m/z* 371.1491 $[M-H]^-$ (calcd for $C_{21}H_{23}O_6$, 371.1500).

3.3.6. (-)-Ganotheaecolumol F (**6**)

Yellow gum; $[\alpha]_D^{24}$ −18.5 (*c* 0.20, MeOH); UV (MeOH) λ_{max} (log ε) 348 (3.27), 254 (3.74), 206 (4.19) nm; ESIMS *m/z* 357 $[M-H]^-$, HRESIMS *m/z* 357.1693 $[M-H]^-$ (calcd for $C_{21}H_{25}O_5$, 357.1707).

3.3.7. (±)-Ganotheaecolumol G (**10**)

Yellow gum; {[α]25D +53.1 (*c* 0.05, MeOH), (+)-**10**; $[\alpha]_D^{25}$ −51.6 (*c* 0.08, MeOH), (-)-**10**}; UV (MeOH) λ_{max} (log ε) 384 (3.24), 254 (3.83), 205 (4.30) nm; ESIMS *m/z* 401 $[M-H]^-$, HRESIMS *m/z* 401.1609 $[M-H]^-$ (calcd for $C_{22}H_{25}O_7$, 401.1606).

3.3.8. (±)-Ganotheaecolumol H (**11**)

Yellow gum; {$[\alpha]_D^{24}$ +10.0 (*c* 0.05, MeOH), (+)-**11**; $[\alpha]_D^{24}$ −4.0 (*c* 0.05, MeOH), (-)-**11**}; UV (MeOH) λ_{max} (log ε) 363 (2.61), 307 (2.96), 224 (3.90) nm; ESIMS *m/z* 385 $[M-H]^-$, HRESIMS *m/z* 385.1659 $[M-H]^-$ (calcd for $C_{22}H_{25}O_6$, 385.1657).

3.3.9. Ganotheaecolumol I (**13**)

Yellow gum; UV (MeOH) λ_{max} (log ε) 373 (3.55), 206 (4.36) nm; ESIMS *m/z* 373 $[M-H]^-$, HRESIMS *m/z* 373.1649 $[M-H]^-$ (calcd for $C_{21}H_{25}O_6$ 373.1657).

3.3.10. Ganotheaecolumol J (**14**)

Yellow gum; UV (MeOH) λ_{max} (log ε) 388 (3.36), 264 (3.85), 227 (4.21) nm; ESIMS *m/z* 371 $[M-H]^-$, HRESIMS *m/z* 371.1489 $[M-H]^-$ (calcd for $C_{21}H_{23}O_6$ 371.1500).

3.3.11. Ganotheaecolumol K (**17**)

Yellow gum; UV (MeOH) λ_{max} (log ε) 361 (3.17), 250 (3.58), 209 (3.92) nm; ESIMS *m/z* 373 $[M-H]^-$, HRESIMS *m/z* 373.1656 $[M-H]^-$ (calcd for $C_{21}H_{25}O_6$ 373.1657).

3.4. Computational methods

The ECD and optical rotation (OR) calculations were performed using a Gaussian 09 program package. The conformational search generating low-energy conformers within a 6 kcal/mol were finished by software Conflex 7. The low-energy conformations were optimized, and ECD and OR calculations were conducted at the B3LYP/6-311G(d,p) level in MeOH, and the results were processed using previously described methods [6].

3.5. Biological assay

3.5.1. Assay for in vitro COX-2 inhibition

The new compounds were evaluated for COX-2 inhibitory activity in vitro by using Cayman's COX Fluorescent Inhibitor Screening Assay Kit (Cayman Chemical Company, Ann Arbor, MI, USA) and a previously described method [22]. The data were analyzed using GraphPad Prism5 software. In this study, celecoxib was used as a positive control with an IC_{50} value of 8.70 ± 0.40 nM.

3.5.2. Assay for in vitro JAK3 kinase inhibition

The inhibitory activity of the new compounds against JAK3 kinase was performed using the FRET-based Z′-Lyte assay system in line with the manufacturer's instructions (Invitrogen, Carlsbad, USA) and a previously described method [19]. The data were analyzed using Graphpad Prism5 software. In this study, staurosporine was used as a positive control with an IC_{50} value of 0.47 ± 0.02 nM.

3.5.3. Assay for cell viability in human cancer cells

Human cancer cell lines including K562, A549, and Huh-7 were obtained from Shanghai Cell Bank, Chinese Academy of Sciences, P.R. China. Cytotoxicity was tested with a previously described method [22]. Concentration response curves were plotted to determine the IC_{50} values using Prism 5.0 software.

Acknowledgments

This work was financially supported by the NSFC-Joint Foundation of Yunnan Province (U1702287), the National Science Fund for Distinguished Young Scholars (81525026), and the National Natural Science Foundation of China (21472199).

Appendix A. Supplementary data

Supplementary data related to this article can be found at https://doi.org/10.1016/j.tet.2018.06.053.

References

[1] Y. Ling, W.G. Hou, Y.R. Dong, B. Lian, S. Yuan, C.C. Dai, Food Sci. 26 (2005) 648–652.
[2] X.L. Chen, J.H. Jia, Y.B. Liu, Modern Food 3 (2016) 65–67.
[3] S.S. Liu, Y. Wang, J. Nanyang Inst. Technol. 7 (2015) 125–128.
[4] X.R. Peng, J.Q. Liu, Z.H. Han, X.X. Yuan, H.R. Luo, M.H. Qiu, Food Chem. 141 (2013) 920–926.
[5] S. Baby, A.J. Johnson, B. Govindan, Phytochemistry 114 (2015) 66–101.
[6] Q. Luo, Z.L. Yang, Y.M. Yan, Y.X. Cheng, Org. Lett. 19 (2017) 718–721.
[7] L.Y. Liu, Z. Yan, J. Kang, R.Y. Chen, D.Q. Yu, J. Asian Nat. Prod. Res. 2 (2017) 1–7.
[8] L.Y. Liu, H. Chen, L. Chao, et al., Fitoterapia 98 (2014) 254–259.
[9] Q. Luo, Z.C. Tu, Z.L. Yang, Y.X. Cheng, Fitoterapia 125 (2018) 273–280.
[10] X.Q. Chen, L.X. Chen, S.P. Li, J. Zhao, Phytochem. Lett. 22 (2017) 214–218.
[11] W.W. Cao, Q. Luo, Y.X. Cheng, S.M. Wang, Fitoterapia 110 (2016) 110–115.
[12] X.M. Niu, S.H. Li, H.D. Sun, C.T. Che, J. Nat. Prod. 69 (2006) 1364–1365.
[13] X.R. Peng, J.Q. Liu, C.F. Wang, et al., Food Chem. 171 (2015) 251–257.
[14] K. Wang, L. Bao, K. Ma, et al., Eur. J. Med. Chem. 127 (2017) 1035–1046.
[15] H.W. Liu, K. Wang, L. Bao, J.J. Han, PCT Int. Appl. WO (2018), 2018014660.
[16] S.Z. Huang, B.H. Cheng, Q.Y. Ma, et al., RSC Adv. 6 (2016) 21139–21147.
[17] Q. Luo, X.H. Yang, Z.L. Yang, Z.C. Tu, Y.X. Cheng, Tetrahedron 72 (2016) 4564–4574.
[18] Q. Luo, X.L. Wang, L. Di, et al., Tetrahedron 71 (2015) 840–845.
[19] Q. Luo, Z. Wang, J.F. Luo, Z.C. Tu, Y.X. Cheng, RSC Adv. 7 (2017) 38037–38043.
[20] Y.M. Yan, J. Ai, L.L. Zhou, et al., Org. Lett. 15 (2013) 5488–5491.
[21] Y.M. Yan, X.L. Wang, L.L. Zhou, et al., J. Ethnopharm. 176 (2015) 385–393.
[22] J.F. Wang, X.Y. Wei, X. Lu, et al., Tetrahedron 70 (2014) 9695–9701.